Nonequilibrium Phase Transitions in the Extraction of Membrane Tubes by Molecular Motors

J. Tailleur,[1] M. R. Evans,[1] and Y. Kafri[2]

[1]SUPA, School of Physics and Astronomy, University of Edinburgh, Mayfield Road, Edinburgh EH9 3JZ, Scotland
[2]Department of Physics, Technion, Haifa, 32000, Israel

(Received 4 December 2008; published 20 March 2009)

The extraction of membrane tubes by molecular motors is known to play an important role for the transport properties of eukaryotic cells. By studying a generic class of models for the tube extraction, we discover a rich phase diagram. In particular we show that the density of motors along the tube can exhibit shocks, inverse shocks, and plateaux, depending on parameters which could in principle be probed experimentally. In addition the phase diagram exhibits interesting reentrant behavior.

DOI: 10.1103/PhysRevLett.102.118109 PACS numbers: 87.16.A−, 05.40.−a, 64.60.−i, 87.16.Nn

Molecular motors play a fundamental role in intracellular traffic [1], being responsible for the transport of vesicles and the extraction of membrane nanotubes [2]. The latter phenomenon is of particular interest as it requires a cooperative effort between many motors. This remarkable collective behavior has been demonstrated *in vitro* only very recently [2], triggering much interest in the features of the "tubulation," with a particular focus on the dynamics of the tip region. Objects of study include the conditions for the formation of tubes, their velocities, the load exerted on and by the motors, the distribution of motors along the tube, and the role of processivity [2–5]. *In vitro*, a tube can be created when a vesicle coated with kinesins is brought near a microtubule [2]. It is generally believed [3] that two regimes are then observed depending on the motor density: below a critical density, the motors which bind to the microtubule are not able to extract a tube; above the critical density tubulation occurs and the motors pull a tube out of the vesicle, at steady velocity. During this process motors constantly bind and unbind from the microtubule, while remaining bound to the membrane (see Fig. 1). In this regime, the density of motors is predicted to be flat, with some structure near the tip region [3]. The critical density and the velocity of the tube have been shown to be very sensitive to details of the tip region, such as the number of motors clustered there and their coordination [6].

In this Letter, on the other hand, we focus on the regime where tubulation is established and study the collective behavior of motors in the bulk of the system. We consider a generic model of two coupled lattices representing bound and unbound motors. By accounting for excluded volume interactions, neglected in [3], we discover a richer phase diagram than previously expected. The tubulation regime now divides into two different phases with reentrant transitions between them. Both phases could in principle be accessible to experiment by control of the vesicle density. As we show, the phase diagram is governed by the bulk dynamics and the effective tip velocity; it is thus insensitive to the precise details of the dynamics of the tip region.

We first describe the phenomenology predicted by our study. The motor density profile comprises two plateaux emerging from the tip of the tube and the vesicle, respectively. These plateaux meet in the bulk of the system which leads to a discontinuity—a kink—in the density profile. The system can be in two different phases, illustrated in Fig. 2: (i) a *kink* phase, in which the tip density is either larger or smaller than that of the vesicle, the two plateaux being connected accordingly by a shock or an inverse shock in the bulk of the system, and (ii) a *tip* phase where the kink travels toward the vesicle and localizes in its vicinity, thus yielding a constant density profile corresponding to the tip density. Apart from a carefully chosen set of parameters, the kink is never at rest, always traveling away from the tip of the tube and either toward (tip phase) or away from the vesicle (kink phase). In the latter case, the kink moves away from both boundaries, which is possible because the tube is extending. The transition between the two different phases, and also the transition from "shock" profile to "inverse-shock" profiles within the kink phase, can be triggered, for instance, by changing the value of the vesicle's density (see the phase diagrams in Fig. 2). Furthermore, the phase diagram is reentrant: by continuously increasing the vesicle's density, one can go from the

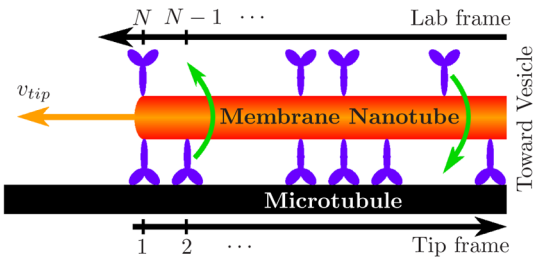

FIG. 1 (color online). Illustration of tube extraction. Molecular motors are attached to the membrane and can bind and unbind from the microtubule. Two frames of reference are used in the text: the "tip frame" is comoving with the tip, with site labels increasing toward the vesicle; the "lab frame" where the vesicle is stationary and the site labels increase towards the tip.

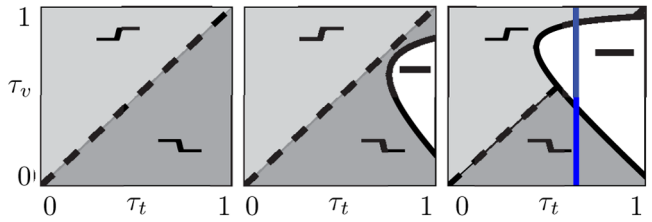

FIG. 2 (color online). Possible phase diagrams depending on the value of the ratio d/a of detachment to attachment rate. The axes represent the densities (τ_t, τ_v) of bound motors in the tip and vesicle plateaux. (a) $1/4 \leq d/a$. The system presents either shock or inverse-shock profiles. (b) $1/8 < d/a < 1/4$. The tip phase appears inside the shock region. (c) $d/a \leq 1/8$. The boundary of the tip phase moves into the inverse-shock region. In cases (b) and (c), reentrant transitions are possible, e.g., along the vertical blue (or gray) line.

kink phase to the tip phase and back again into the kink phase.

In nonequilibrium statistical physics, shocks play an important role for driven lattice gas models [7] but the phenomenology described here differs from previously studied biophysical traffic problems [8]; reentrance is unusual and previously observed *inverse* shocks required slow particles, static defects, or special current-density relations [9].

Definition of the model.—The microscopic details of the model are as follows (see Fig. 3). We consider two coupled one-dimensional lattices, for bound and unbound motors, which extend from the vesicle to the tip of the tube. A motor bound to the microtubule steps toward the tip of the tube at rate p, provided the arrival site is empty. Each site of the unbound motor lattice accounts for a whole perimeter of the tube, which in experiments exceeds 100 nm [2] and can contain many motors. For the sake of clarity we thus neglect the exclusion on this lattice and assume that unbound motors diffuse freely at rate D. Partial exclusion could be taken into account: for realistic values of the parameters (see below), it does not modify qualitatively the phase diagram and just obscures the algebra [10]. Finally, motors attach at rate a to an empty site and detach at rate d from the microtubule.

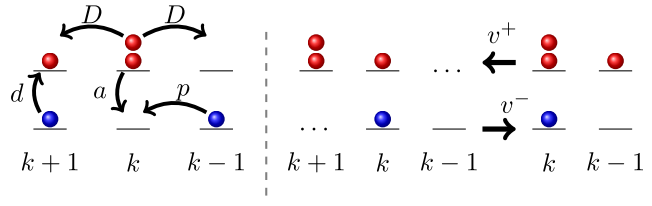

FIG. 3 (color online). Coupled lattice model for the bulk dynamics. The sites are labeled in the lab frame. The bottom and top lattices represent bound and unbound motors, respectively. Possible transitions of motors in the bulk are illustrated by arrows in the left panel. The right panel shows how extension and retraction of the tube drag the unbound motors in the bulk.

A complete description of the tube dynamics would also include the details of the dynamics in the vicinities of the tip and the vesicle. As shown numerically in [6], these details are important for establishing the conditions for tubulation. However, as demonstrated below, the form of the phase diagram is insensitive to these details and relies on the fact that the tube has a well-defined mean velocity during tubulation. We thus posit that extension and retraction events occur with rates v^+ and v^-, yielding a tube velocity $v_{\text{tip}} = v^+ - v^-$. Also, since the viscosity of the membrane is 2 orders of magnitude larger than that of the buffer [3], the unbound motors are dragged every time the tube extends or retracts (see Fig. 3). Under these conditions our results encompass a whole class of models for the tube dynamics including, for instance, those considered in [6]. We now derive the different phases within a mean-field analysis.

Mean-field (MF) theory.—In the analysis that follows it will be useful to consider two distinct frames of reference: the lab frame, where the vesicle is stationary and the site labeling starts at the vesicle and increases toward the tip of the tube; the tip frame, which is comoving with the tip of the tube, and where the site labeling starts at the tip and increases toward the vesicle (see Fig. 1). In the tip frame, the mean-field equations read

$$\dot{\tau}_i = -J_i^b + J_{i-1}^b + K_i; \qquad \dot{\sigma}_i = -J_i^u + J_{i-1}^u - K_i. \tag{1}$$

Here, τ_i and σ_i are the average occupancies of bound and unbound motors at site i. The current of bound motors moving between sites $i+1$ and i is given by $J_i^b = -p(1-\tau_i)\tau_{i+1} + v^+\tau_i - v^-\tau_{i+1}$ whereas the current of unbound motors reads $J_i^u = -D[\sigma_{i+1} - \sigma_i]$. Both currents are defined to be positive in the direction of increasing i, i.e., when they transport motors *away* from the tip. Also, in the tip frame, extension and retraction of the tube affects the bound motors throughout the lattice, whence the contribution of v^+ and v^- to J_i^b. Last, $K_i = a\sigma_i(1-\tau_i) - d\tau_i$ is the flux of motors between the two lattices. The counterpart of these equations in the lab frame (i increasing toward the tip) is easily obtained:

$$\dot{\tau}_i = -j_i^b + j_{i-1}^b + K_i; \qquad \sigma_i = -j_i^u + j_{i-1}^u - K_i, \tag{2}$$

where $j_i^u = -D(\sigma_{i+1} - \sigma_i) + v^+\sigma_i - v^-\sigma_{i+1}$ and $j_i^b = p\tau_i(1-\tau_{i+1})$ are the unbound and bound currents. Here also, currents are positive in the direction of increasing i.

As we now show, the velocity of the tip of the tube selects plateau densities of bound and unbound motors, which we call τ_t and σ_t, respectively. At the other end, the density of motors on the vesicle selects in general different plateau densities which we call τ_v and σ_v. To derive the steady-state plateau densities, we assume constant $\tau_{t,v}$ and $\sigma_{t,v}$ in either (1) or (2). This yields a zero flux between the two lattices $K_i = 0$, implying for any pair of plateau densities τ and σ

$$\sigma = d\tau/[a(1-\tau)]. \quad (3)$$

Let us first consider the tip plateau values τ_t and σ_t using Eq. (1). Adding upper and lower lattice contributions yields a conservation equation for the total flux

$$F_t \equiv J_i^b + J_i^u = 0. \quad (4)$$

The total flux F_t flowing through the tip plateau in the tip frame has to equal zero as nothing can move to the left of site 1. Using the explicit expressions of J_i^b and J_i^u in (4) and relation (3) yields

$$\tau_t = 1 - \frac{v_{\rm tip}}{p}; \qquad \sigma_t = \frac{d}{a}\left(\frac{p}{v_{\rm tip}} - 1\right). \quad (5)$$

Note that we do not specify equation (or dynamics) near the tip region. Solving such equations will give (generally complicated) relations between the rates at tip region and values of $v_{\rm tip}$, τ_t, and σ_t while leaving Eq. (5) unmodified. They will therefore not influence our results.

The vesicle plateau, however, is determined by the density of motors on the vesicle and the details of the nearby dynamics. While such equations can be solved for specific models, to analyze the phase diagram it is enough to know that τ_v can take any value between 0 and 1.

Tip and vesicle plateau densities are typically different which suggests the possibility of a kink phase with shock and inverse-shock profiles when $\tau_t > \tau_v$ and $\tau_t < \tau_v$ respectively. Generally, the kink is not at rest and this phase disappears if it propagates to either end of the system. To analyze this, we consider the kink velocity in the tip frame v_t^k and in the lab frame v_l^k. Conservation of mass implies $v_t^k = (F_t - F_v)/(\rho_t - \rho_v)$, where $F_{t,v}$ and $\rho_{t,v} = \tau_{t,v} + \sigma_{t,v}$ are the *total* fluxes and densities to the left and right of the kink, in the tip frame. F_v reads $F_v = -p(1-\tau_v)\tau_v + v_{\rm tip}\tau_v$. Using (3) and (5) to eliminate $\sigma_{t,v}$ and $v_{\rm tip}$, we obtain v_t^k in terms of $\tau_{t,v}$:

$$v_t^k = \frac{p\tau_v(1-\tau_t)(1-\tau_v)}{(1-\tau_t)(1-\tau_v) + d/a}. \quad (6)$$

In the lab frame, the kink velocity is $v_l^k = v_{\rm tip} - v_t^k$:

$$v_l^k = p(1-\tau_t) - \frac{p\tau_v(1-\tau_t)(1-\tau_v)}{(1-\tau_t)(1-\tau_v) + d/a}. \quad (7)$$

Since $\tau_{t,v}$ are smaller than 1, v_t^k is necessarily positive; i.e., the kink always propagates away from the tip. Transposed in the lab frame, this means that the kink never catches up with the tip. However, v_l^k can be negative; i.e., the kink may not propagate away from the vesicle. The tip phase indeed occurs when the kink is localized at the vesicle and the density then equals that of the tip plateau, except in a boundary layer close to the vesicle.

The tip phase thus requires $v_l^k < 0$, which reads $(1-\tau_v)(1-\tau_v-\tau_t) + d/a < 0$ and can only be satisfied if

$$\tau_t > 2\sqrt{d/a}. \quad (8)$$

The system is then in the tip phase for $\tau_v \in [\tau_-; \tau_+]$, where

$$\tau_\pm = 1 - \frac{\tau_t}{2} \pm \frac{\sqrt{\tau_t^2 - 4d/a}}{2}. \quad (9)$$

When τ_v is not in $[\tau_-; \tau_+]$ or condition (8) is not met, the system is in the kink phase, presenting shock when $\tau_t > \tau_v$ or inverse shock when $\tau_t < \tau_v$. Note that for $\tau_t \in [0, 1]$, one always has $\tau_- > 0$ and $\tau_+ < 1$. The phase diagram thus always exhibits reentrance if $d/a < 1/4$; i.e., values of τ_t always exist for which a continuous increase of τ_v drives the system from the kink phase into the tip phase and back into the kink phase. We present the various possible phase diagrams in Fig. 2.

Numerics.—In order to validate the theoretical predictions, we now turn to simulations of a concrete model within the class considered here. The bulk dynamics has already been described (see Fig. 3) and we now specify dynamics in the vicinity of the tip and the vesicle. Our interest lies in verifying the phase diagram and to this end we choose a particularly simple model. The vesicle is represented by reservoirs of bound and unbound motors of densities τ_0 and σ_0. For simplicity, they are chosen to satisfy (3) so that there is no flux between them [11]. At the other end, the tube extends at rate γ by one lattice site if a bound motor occupies the site next to the tip. When this happens, the new unbound site next to the vesicle is equilibrated with the reservoir of density σ_0. If a bound motor does not occupy the site next to the tip the tube retracts with rate μ. At this site motors can still attach and detach with rates a and d and unbound motors can hop toward the vesicle, with rate D. At long times, this tip dynamics yields average extension and retraction rates $v^+ = \gamma\tau_1$ and $v^- = \mu(1-\tau_1)$.

Models aiming to predict the threshold for tubulation and tube velocity would require modified attachment and detachment rates at the site closest to the tip and should

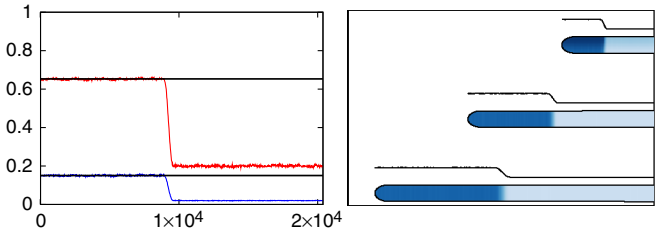

FIG. 4 (color online). Shock profiles obtained from numerics ($p = 1$, $d = .08$, $a = 1$, $D = 1$, $\mu = 9$, $\gamma = 0.45$, $\tau_0 = 0.2$). Data are averaged over a short time window ($\Delta t = 1000$) and then over 100 simulations. Left panel: Bound (upper) and unbound (lower) motor densities along the tube, in the tip frame, at time $t = 60\,000$. Black lines correspond to MF predictions (5), with $v_{\rm tip}$ obtained from the simulation. Right panel: Density of motors (black) at fixed time intervals ($t = 4 \times 10^4$; 8×10^4; 12×10^4) in the lab frame. Tubes are color-coded, with light and dark blue (or gray) representing low and high density. Note that the tip moves faster than the shock.

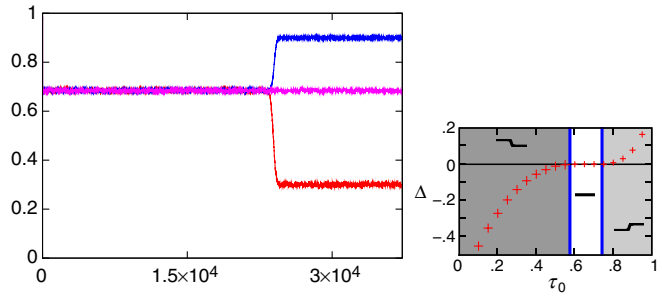

FIG. 5 (color online). Left panel: Different profiles are illustrated as in Fig. 4, but with $t = 120\,000$, $d = 0.11$, and $\tau_0 = 0.3$, 0.6, 0.9. Note that the length of the lattice, hence the tube velocity, is independent of τ_0. Right panel: Numerical value of Δ (crosses) along the vertical blue (or gray) line of Fig. 2. When τ_0 goes from 0 to 1, the average density of bound motors is first lower than that of the tip plateau ($\Delta < 0$, shock), then equals it ($\Delta = 0$, tip phase), and last overcomes it ($\Delta = 0$, inverse shock). The vertical blue (or gray) lines correspond to the predicted boundaries of the tip phase (9). There is thus a reentrant phase transition from the kink phase to the tip phase and back into the kink phase, whose boundaries are accurately predicted by the MF theory.

account for backward stepping there. However, as noted above, the phase diagram depends only on the tip velocity and not on further details of the tip dynamics.

We now consider the results of continuous time simulations of the model. In Fig. 4, a typical shock profile and its dynamics are presented. Note the quantitative agreement with the predictions of the mean-field theory.

We have also verified the general structure of the phase diagram and present results for the blue line indicated in Fig. 2. The different profiles observed are presented in Fig. 5. From previous lattice gas studies, one would expect the inverse shock to smooth out through a rarefaction fan. Here, on the other hand, we checked numerically that its relative width vanishes in the large time limit; it is thus stabilized by the interaction of the two lattices [10]. The figure also shows that the tip velocity is independent of τ_v, once tubulation is established. A mean-field analysis [10] suggests that this holds for generic local tip dynamics.

To quantify the transition, we define $\Delta = \sum_i \tau_i/L - \tau_t$, where L is the length of the tube. This compares the average mass of bound motors in the system with that of a putative tip phase. The parameter Δ is nonzero in the kink phase and zero in the tip phase. An example of reentrance is shown in Fig. 5. Starting with τ_0 close to 0, we see that Δ is negative, vanishing at $\tau_0 = \tau_-$ where the system enters the tip phase. A further increase of τ_0 above $\tau_0 = \tau_+$ drives the system back into the kink phase, in the inverse-shock region, and Δ becomes positive.

Conclusion.—In this Letter we have shown that the dynamics of tubulation reveals a rich phenomenology, including shocks, inverse shocks, and reentrant phase transitions. This arises from the two competing densities set by the two ends of the tube and the dynamics of the resulting kink determines the phase structure. This picture is substantiated by a mean-field theory which accurately predicts the phase diagram, as checked by our numerics.

Some experimental signatures of our theory are as follows. First, the velocity of the tip should always exceed that of the kink. Also, once tubulation is established, the velocity of the tip is not sensitive to the density of motors on the surface of the vesicle. Last, in the experiment, the ratio $d/a \simeq 0.1$ is very small [6]. It should therefore be possible to observe the transitions to the tip phase by varying the density of motors on the surface of the vesicle. To explore the full phase diagram presented in Fig. 2, one needs to change microscopic rates to vary τ_t. Experimentally, this could be done by changing parameters such as the membrane surface tension or the ATP concentration. Finally, corrections to the phase diagram due to partial exclusion among unbound motors is of order $d/aN_{\max}$ where $N_{\max}$ is the maximal occupancy of the unbound lattice [10]. Here, it would be of the order of 0.01.

We thank D. Mukamel for a critical reading of the manuscript. J. T. acknowledges funding from EPSRC Grant No. EP/030173. Y. K. thanks the Israeli Science Foundation for support and O. Campas for discussions.

[1] J. C. Howard, *Mechanics of Motor Proteins and the Cytoskeleton* (Sinauer, Sunderland, MA, 2001).
[2] A. Roux *et al.*, Proc. Natl. Acad. Sci. U.S.A. **99**, 5394 (2002).
[3] C. Leduc *et al.*, Proc. Natl. Acad. Sci. U.S.A. **101**, 17096 (2004).
[4] P. M. Shaklee *et al.*, Proc. Natl. Acad. Sci. U.S.A. **105**, 7993 (2008).
[5] O. Campas *et al.*, Phys. Rev. Lett. **97**, 038101 (2006).
[6] O. Campas *et al.*, Biophys. J. **94**, 5009 (2008).
[7] J. S. Hager *et al.*, Phys. Rev. E **63**, 056110 (2001); K. Nishinari *et al.*, Phys. Rev. Lett. **95**, 118101 (2005); R. A. Blythe and M. R. Evans, J. Phys. A **40**, R333 (2007).
[8] Y. Aghababaie, G. I. Menon, and M. Plischke, Phys. Rev. E **59**, 2578 (1999); S. Klumpp and R. Lipowsky, J. Stat. Phys. **113**, 233 (2003); A. Parmeggiani, T. Franosch, and E. Frey, Phys. Rev. Lett. **90**, 086601 (2003); D. Chowdhury, A. Schadschneider, and K. Nishinari, Phys. Life Rev. **2**, 318 (2005); S. A. Nowak, P. W. Fok, and T. Chou, Phys. Rev. E **76**, 031135 (2007); K. E. P. Sugden *et al.*, Phys. Rev. E **75**, 031909 (2007); K. Tsekouras and A. B. Kolomeisky, J. Phys. A **41**, 465001 (2008); H. Grzeschik, R. J. Harris, and L. Santen, arXiv:0806.3845.
[9] J. Krug, Phys. Rev. Lett. **67**, 1882 (1991); M. R. Evans, Europhys. Lett. **36**, 13 (1996); K. Mallick, J. Phys. A **29**, 5375 (1996); A. B. Kolomeisky, J. Phys. A **31**, 1153 (1998).
[10] J. Tailleur, M. R. Evans, and Y. Kafri (to be published).
[11] For generic rates, a finite size boundary layer is formed.